Electron Transfer from the Acceptor A_1 to the Iron–Sulfur Centers in Photosystem I As Studied by Transient EPR Spectroscopy†

Arthur van der Est,*,‡ Christian Bock,‡ John Golbeck,§ Klaus Brettel,∥ Pierre Sétif,∥ and Dietmar Stehlik‡

Fachbereich Physik, Freie Universität Berlin, Arnimallee 14, 14195 Berlin, Germany, Department of Biochemistry, University of Nebraska, Lincoln, Nebraska 68583-0718, and Section de Bioénergétique CNRS, URA 1290, Département de Biologie Cellulaire et Moléculaire, CEA-Saclay, 91191 Gif-sur-Yvette Cedex, France

Received March 10, 1994; Revised Manuscript Received June 23, 1994®

ABSTRACT: The electron transfer in photosystem I (PS I) from the secondary acceptor A_1 to the iron–sulfur centers is studied by X-band transient EPR with a time resolution of ~50 ns. Results are presented for a series of different PS I preparations from the cyanobacterium *Synechococcus* 6301 ranging from whole cells to core particles in which the iron–sulfur centers have been successively removed. In addition, results from PS I preparations from spinach and the cyanobacterium *Synechocystis* 6803 are presented. In all samples containing iron–sulfur centers, two consecutive spin-polarized EPR spectra are observed. The two signals have previously been assigned to the charge-separated states $P_{700}^{+\bullet}A_1^{-\bullet}$ and $P_{700}^{+\bullet}(FeS)^-$, where (FeS) is one of the three iron–sulfur centers, F_X, F_A, or F_B [Bock, C., van der Est, A., Brettel, K., & Stehlik, D. (1989) *FEBS Lett. 247*, 91–96]. In agreement with this, the second spectrum is not observed in the sample in which the iron–sulfur centers have been removed. For (P_{700}-F_X), core particles which do not contain F_A and F_B, the second spectrum can unambiguously be assigned to the pair $P_{700}^{+\bullet}F_X^-$. In all samples containing F_X, the transition from the first to the second spectrum occurs with $t_{1/e} \approx 280$ ns ($t_{1/2} \approx 190$ ns) both in the presence and absence of F_A and F_B, which strongly suggests that this phase reflects electron transfer from $A_1^{-\bullet}$ to F_X in intact PS I. For the spinach particles and for the cyanobacterial (P_{700}-F_X) core particles, the EPR data show evidence for the presence of a fraction of the reaction centers in which electron transfer from $A_1^{-\bullet}$ to F_X is faster than the response time of the spectrometer, in agreement with optical data for the same samples. It is shown that when this fraction is taken into account the early spectrum extracted from the EPR data sets shows no net spin polarization and is identical for all samples except the (P_{700}-A_1) core particles. Possible reasons for the differences in this sample are discussed.

The initial steps in the photosynthetic electron transport in photosystem I (PS I)[1] have been studied extensively (Golbeck, 1992; Sétif, 1992; Lagoutte & Mathis, 1989; Andreasson & Vänngard, 1988). Spectroscopic studies show that excitation of the primary donor, P_{700}, leads to the transfer of an electron to the protein bound acceptors A_0, A_1, F_X, F_A, and F_B, where P_{700} is a chlorophyll *a* dimer analogous to the special pair in bacterial reaction centers, A_0 is a chlorophyll *a* monomer, A_1 is phylloquinone, and F_X, F_A, and F_B are [4Fe-4S] clusters. The pathway and kinetics of the electron transfer have not yet been firmly established. The involvement of A_0 as an intermediate between P_{700} and A_1 has been placed in doubt by recent transient absorption and fluorescence results with picosecond resolution in which no significant population of A_0^- could be detected (Holzwarth et al., 1993). Conclusive evidence that the acceptor A_1 is phylloquinone has been obtained from quinone exchange experiments using transient EPR at low temperature (Rustandi et al., 1990; Stehlik et al., 1993; Rustandi et al., 1992) and room temperature (Sieckmann et al., 1991). This is substantiated by the fact that the CW EPR spectrum attributed to $A_1^{-\bullet}$ disappears when A_1 is doubly reduced (Snyder et al., 1991; Heathcote et al., 1993). The first acceptor following A_1 is one of the three iron–sulfur centers, F_X, F_A, or F_B. It is usually identified as F_X, which is supported by EPR and optical data from (P_{700}-F_X) core particles which show that electron transfer to F_X occurs in the absence of F_A and F_B (Warden & Golbeck, 1986; Golbeck & Cornelius, 1986; Golbeck et al., 1987; Lüneberg et al., 1994). Previous measurements (Mathis & Sétif, 1989; Brettel, 1989; Bock et al., 1989) of the rate for the electron transfer step $P_{700}^{+\bullet}A_1^{-\bullet} \rightarrow P_{700}^{+\bullet}(FeS)^-$ yielded conflicting results. Transient optical absorption difference spectroscopy on PS I particles from spinach gave $t_{1/2} = 25$ ns ($t_{1/e} = 36$ ns) (Mathis & Sétif, 1989) whereas a value of $t_{1/2} = 200$ ns ($t_{1/e} = 290$ ns) was obtained from optical (Brettel, 1989) and transient EPR studies (Bock et al., 1989) of PS I particles from the cyanobacterium *Synechococcus* sp. and spinach chloroplasts. More recent transient optical absorption measurements (Sétif & Brettel, 1993) show that this apparent contradiction is a result of differences in the preparation of the samples. It was found that the reoxidation of $A_1^{-\bullet}$ is essentially monophasic with $t_{1/2} = 200$ ns ($t_{1/e} = 290$ ns) in PS I from cyanobacteria, in agreement with earlier studies. However, in spinach PS I particles, the reoxidation was found to be generally biphasic with time constants of $t_{1/2} = 25$ ns ($t_{1/e} = 36$ ns) and $t_{1/2} = 150$ ns ($t_{1/e} = 215$ ns) with the relative amounts of the two

† This work was supported by grants from the Deutsche Forschungsgemeinschaft (Sfb 312, Teilprojekte A1 and A5), an EMBO fellowship to P.S., and a grant from the U.S. National Science Foundation (DMB-9205756) to J.G.

* Author to whom correspondence should be addressed.
‡ Freie Universität Berlin.
§ University of Nebraska.
∥ Section de Bioénergétique CNRS.

® Abstract published in *Advance ACS Abstracts,* September 1, 1994.

[1] Abbreviations: PS I, photosystem I; P_{700}, primary electron donor of PS I; A_1, primary quinone acceptor in PS I; VK_1, vitamin K_1; FeS, iron–sulfur center; F_A, F_B, and F_X, the [4Fe-4S] iron–sulfur clusters of PS I; RC, reaction center; DM, β-dodecyl maltoside; EPR, electron paramagnetic resonance; ESP, electron spin polarization; RP, radical pair; A, absorption; E, emission; Chl, chlorophyll.

0006-2960/94/0433-11789$04.50/0

components being very dependent on the method of preparation. A kinetic scheme consistent with the results was proposed (Sétif & Brettel, 1993) in which the 25 ns component is attributed to electron transfer from $A_1^{-\bullet}$ to F_X. However, the precise nature of the electron transfer step governed by the slower time constant is uncertain. More importantly, it is not apparent what causes the difference in the electron transfer kinetics between different PS I preparations and how relevant the data are for unperturbed reaction centers, although the authors suggest that the longer of the two time constants probably applies. Clearly, further work is needed to help clarify this, and a thorough investigation of the differences in the kinetic and spectroscopic data for PS I under different experimental conditions is necessary.

In this paper we will examine the transient EPR results for various PS I preparations. Under physiological conditions, two sequential spin-polarized transient EPR spectra are observed which can be assigned to the radical pairs $P_{700}^{+\bullet}A_1^{-\bullet}$ and $P_{700}^{+\bullet}(FeS)^-$ (Bock et al., 1989). At low temperatures the second spectrum is not present presumably because electron transfer to the iron–sulfur centers is irreversible under these conditions (Malkin & Bearden, 1971) and only those RC's in which recombination from A_1 occurs are observed. For this reason only room temperature results will be presented.

Our primary goal here is to identify which of the three iron–sulfur centers accepts the electron from the phylloquinone following the creation of the charge separated state $P_{700}^{+\bullet}A_1^{-\bullet}$. In principle, the electron spin polarization (ESP) patterns of two sequential radical pairs contain a great deal of information about the species involved (for reviews see Hore, 1989; Bixon et al., 1992; Snyder & Thurnauer, 1993). Extracting this information from the second spectrum is complicated by the fact that the ESP pattern results from a projection of the polarization in the first radical pair onto the spin states of the second pair (Bock, 1989; Norris et al., 1990). The interpretation of the $P_{700}^{+\bullet}(FeS)^-$ spectrum has the additional complication that the contribution from $(FeS)^-$ is not observed because the large anisotropy in its *g*-tensor distributes the intensity over a very large field range. Thus, rather than attempting to obtain information about the iron–sulfur acceptor from a spectral analysis, we will investigate changes in the spin-polarized EPR signals which are a result of systematically shortening the chain of electron acceptors beyond A_1. An important advantage of the EPR method for such studies is that it can be used on completely intact systems the high optical density and light scattering of which make transient optical measurements very difficult. Because the electron transfer in PS I is the only photoinduced process in these systems which produces spin-polarized EPR signals, there is no interference from PS II or other parts of the sample. We will begin by comparing the results for cyanobacteria and spinach samples at various steps during the PS I isolation procedure as well as for samples in which the forward electron transfer to the iron–sulfur centers has been partially blocked by removal of the PsaC protein unit which contains F_A and F_B or completely blocked by the subsequent denaturation of F_X. Transient optical absorption studies on similar samples (Lüneberg et al., 1994) show that the $t_{1/e}$ = 290 ns ($t_{1/2}$ = 200 ns) phase attributed to the oxidation of $A_1^{-\bullet}$ is still observed when F_A and F_B are absent. This strongly suggests that this phase should be assigned to the electron transfer from $A_1^{-\bullet}$ to F_X. We will show that the EPR results support this assignment and indicate that this electron transfer step occurs in fully intact PS I. We will also show that the EPR spectra of several of the PS I particle samples indicate the presence of a $t_{1/2} < 50$ ns ($t_{1/2} < 35$ ns) kinetic phase in the electron transfer past A_1^- but that such a phase is not observed in the more intact samples such as chloroplasts and thylakoid membranes.

MATERIALS AND METHODS

Growth of Cyanobacterial Strains. *Synechococcus* sp. PCC 6301 was grown in Krantz and Myers medium C (Kratz & Myers, 1955) at 38 °C under continuous fluorescent (cool white) illumination at 60 $\mu E/m^2/s$. Cultures were aerated continuously with 5% CO_2 in air and harvested by hollow fiber membrane filtration (Amicon DC10L) in late log growth at a density corresponding to 15 μg of Chl/mL. *Synechocystis* sp. PCC 6803 was grown in BG-11 medium at 34 °C under the same conditions, except that the cells were aerated without supplemental CO_2. The harvested cells were pelleted by centrifugation and resuspended to 0.3–0.6 mg/mL Chl in 30 mM phosphate buffer, pH 7.6, containing 3 mM EDTA; 0.1% (1 g/L) of egg white lysozyme was added; and the cells were stirred overnight at 20 °C. All subsequent steps were performed at 4 °C.

Preparation of Thylakoid Membranes. The *Synechococcus* sp. PCC 6301 cells were broken by sonication (Branson Model S125); the *Synechocystis* sp. PCC 6803 cells were broken in a bead beater (Biospec Products, Bartlesville, OK). The broken cells were layered onto 0.5 M sucrose, 10 mM EDTA, and 50 mM Tris, pH 8.3, in a 2:3 volume ratio and centrifuged for 60 min at 20 000 rpm (SS-34 rotor, 48000*g*). The pellet was resuspended in 30 mM phosphate buffer, pH 7.6, containing 3 mM EDTA and stored at −80 °C until needed. This sample represents the purified thylakoid membranes.

Preparation of (P_{700}-F_A/F_B) DM and (P_{700}-F_A/F_B) Triton X-100 Particles. The thawed membranes were pelleted by centrifugation for 60 min at 20 000 rpm and resuspended in 30 mM β-dodecyl maltoside (DM) or 1% Triton X-100 containing 0.2 M KCl and 50 mM Tris buffer, pH 8.3. The samples were incubated for 24 h at 4 °C and centrifuged for 60 min at 15 000 rpm. The supernatant was concentrated by ultrafiltration (Amicon YM-100), loaded onto a 0.1–1 M sucrose gradient containing 50 mM Tris buffer, pH 8.3, and either 30 mM DM or 0.1% Triton X-100, and ultracentrifuged for 48 h at 25 000 rpm (SW-27 rotor, 113000*g*). The lower band was dialyzed against 50 mM Tris, pH 8.3, for 12 h, concentrated to 30 mL volume by ultrafiltration, and ultracentrifuged in a sucrose gradient under the same conditions. The lower band, which contains the PS I and cofactors P_{700}, A_0, A_1, F_X, F_B, and F_A, was dialyzed against 50 mM Tris buffer, pH 8.3, concentrated to 1 mg/mL Chl by ultrafiltration, and stored at −80 °C in 20% (v/v) glycerol. This sample represents the (P_{700}-F_A/F_B) DM or Triton X-100 particles.

Preparation of F_A/F_B-Depleted (P_{700}-F_X) Core Particles. The Triton X-100 particles were incubated with 6.8 M urea at 250 μg Chl/mL to remove the PsaC, PsaD, and PsaE proteins (Parrett et al., 1989, 1990). The progress of the reaction was monitored by measuring the loss of the F_A and F_B clusters using optical flash photolysis. After typically 10–15 min, when the 30 ms backreaction between $P_{700}^{+\bullet}$ and $[F_A/F_B]^-$ was entirely replaced by the ~1 ms backreaction between P_{700}^+ and F_X^-, the reaction was quenched by addition of 5 volumes of 50 mM Tris, pH 8.3. The diluted sample was dialyzed overnight against 50 mM Tris, pH 8.3, concentrated by ultrafiltration, and centrifuged for 18 h at 113000*g* (SW-27 rotor) in a 0.1–1 M sucrose gradient containing 50 mM Tris, pH 8.3, and 0.04% Triton X-100. The lower green band,

which contains the PS I and cofactors P_{700}, A_0, A_1, and F_X, was removed, dialyzed against 50 mM Tris, pH 8.3, and stored at −80 °C in 20% glycerol. This sample represents the (P_{700}-F_X) core particle.

Preparation of F_X, F_B, and F_A-Depleted (P_{700}-A_1) Core Particles. The F_X cluster was removed by incubating the P_{700}-F_X core particle at 100 μg/mL Chl for 3 h with 3 M urea and 5 mM $K_3Fe(CN)_6$ in 50 mM Tris, pH 8.3 (Warren et al., 1990, 1993). The progress of the reaction was monitored by measuring the loss of the F_X cluster using optical flash photolysis. When the 1 ms backreaction between $P_{700}^{+\bullet}$ and F_X^- was entirely replaced by the 10 μs backreaction between $P_{700}^{+\bullet}$ and $A_1^{-\bullet}$, the reaction was quenched by addition of 5 volumes of 50 mM Tris, pH 8.3. The diluted sample was dialyzed overnight against 50 mM Tris, pH 8.3, containing 5 mM Tiron, and the iron–Tiron chelate was removed by dialysis for 12 h in 50 mM Tris, pH 8.3, and 0.04% Triton X-100 The sample, which contains PS I and the cofactors P_{700}, A_0, and A_1, was concentrated to 1 mg of Chl/mL by ultrafiltration and stored in 20% glycerol at −80 °C. This sample represents the (P_{700}-A_1) core particle.

Preparation of Spinach Chloroplasts and Particles. The method used to prepare spinach chloroplasts is given by Winget et al. (1965) and the spinach PS I-β particles were prepared as described by Lagoutte et al. (1984).

EPR Experiments. In order to accelerate the otherwise prohibitively slow recombination of the light-induced charge separation, the EPR samples were prepared with 3 mM sodium ascorbate, 80 μM phenazine methosulfate, and 80 mM 2,6-dichlorophenolindophenol as external electron acceptors and donors. The EPR experiments were performed at 9 GHz (X-band) in the direct detection mode using no field modulation. All measurements were taken at room temperature and the sample was pumped continuously through a flat cell during the experiments. The EPR spectrometer, sample cell, and data acquisition procedure are described in more detail by Bock et al. (1989) and Stehlik et al. (1989b). For all samples, a complete time/magnetic field data set was collected with a resolution of 10 ns along the time axis and 0.025 mT along the magnetic field axis as described by Bock et al. (1989). The evaluation of the data set will be discussed in detail below. All spectra and transients presented below are plotted such that absorptive signals (A) are positive and emissive signals (E) are negative.

RESULTS AND DISCUSSION

Figures 1 and 2 show selected transient EPR signals and spectra which have been extracted from the complete data sets for three *Synechococcus* 6301 samples. The traces represent various steps in the isolation and modification of the PS I RC. From top to bottom the samples are (P_{700}-F_A/F_B) DM particles, (P_{700}-F_X) core particles, and (P_{700}-A_1) core particles. The transients correspond to the field position B_0 = 338.8 mT (g = 2.0040), which is marked with an arrow in Figure 2. The details of the fitting procedure used to extract the spectra will be discussed in the next section. Similar results for spinach chloroplasts and PS I-β particles are shown in Figures 3 and 4. In both figures, the chloroplast results are shown at the top and the PS I-β results are shown at the bottom. For these experiments, the electrical bandwidth of the spectrometer was reduced to 10 MHz to improve the signal to noise ratio. The difference in the decay rates of the transients in Figure 3 is due to differences in the microwave power used (see below). As can be seen in these figures, two successive spectra are observed for all samples with the

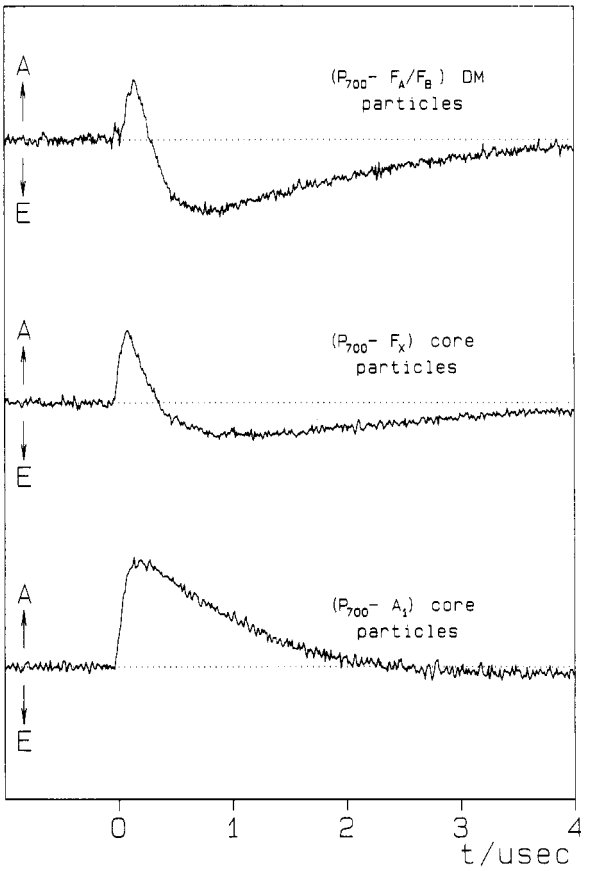

FIGURE 1: Transient EPR signals from PS I in *Synechococcus* 6301 in the region 338.725–338.975 mT. The field position is marked with an arrow in the corresponding spectra shown in Figure 2. From top to bottom: (P_{700}-F_A/F_B) DM particles, (P_{700}-F_X) core particles, and (P_{700}-A_1) core particles. The curves are the averages of 3940, 1280, and 1280 events, respectively. All three transients were recorded at room temperature using 10 mW of microwave power at 9.5045 GHz. The time t = 0 is defined by the leading edge of the 10 ns laser pulse used to excite the sample.

exception of the (P_{700}-A_1) core particles (Figures 1 and 2, bottom). The early spectrum (solid curves) from all samples is dominated by the well-known E/A/E polarization pattern, which has been unambigously assigned to $P_{700}^{+\bullet}$-$A_1^{-\bullet}$ by quinone extraction reconstution experiments (Sieckmann et al., 1991). The late spectrum (dashed curves) which is predominantly emissive has been previously assigned to the charge-separated state $P_{700}^{+\bullet}$-$(FeS)^-$ (Bock et al., 1989) where (FeS) is one of the three iron–sulfur centers. The fact that a late spectrum is still observed when the PsaC protein containing F_A and F_B is removed (Figure 2, middle) but disappears when F_X is removed (Figure 2, bottom) suggests that it should be assigned to $P_{700}^{+\bullet}F_X^-$ and that the rate constant with which it is formed from the early spectrum should be assigned to the electron transfer from $A_1^{-\bullet}$ to F_X. However, inspection of the top and middle traces reveals differences in the relative intensities of the two parts of the transients as well as apparently slower kinetics in the (P_{700}-F_X) core sample.

The results from the two spinach samples shown in Figure 3 clearly demonstrate the effect on the transients of the $t_{1/2}$ = 25 ns phase in the electron transfer from $A1^{-\bullet}$ to FeS as reported for spinach PS I-β particles (Sétif & Brettel, 1993). The presence of such a phase means that for a portion of the RC's the electron has already been transferred to the iron–sulfur centers within the rise time of the spectrometer. For the transients shown in Figures 1 and 3, this results in a decrease in the absorption due to $P_{700}^{+\bullet}A_1^{-\bullet}$ and an increase in the

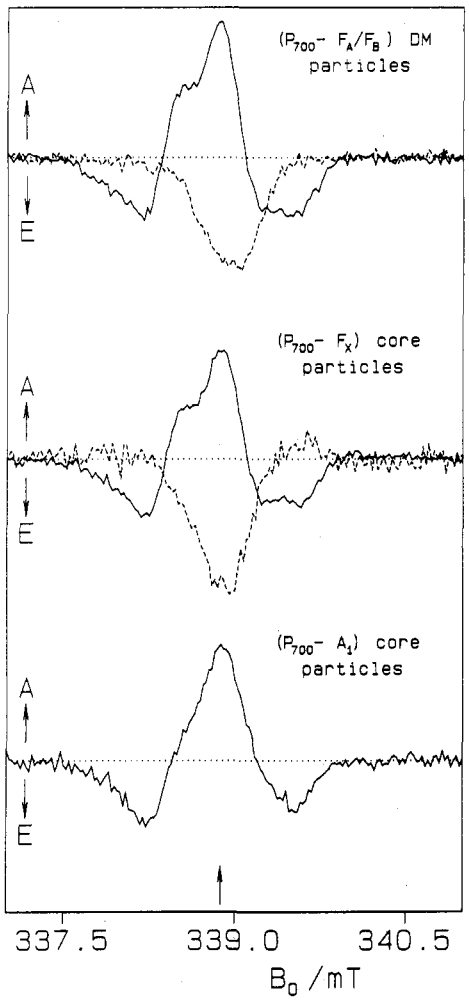

FIGURE 2: Transient EPR spectra derived from the data sets from the same samples as in Figure 1. The arrow indicates the field position for the transients in figure 1. The spectra from top to bottom have been obtained by fitting eq 4 to the respective experimental transients: solid curves, early spectrum $\alpha(B_0)$; dashed curves, late spectrum $\beta(B_0)$. The rate constants used are given in Table 1. The spectrometer response time is 50 ns in all cases. In eq 4 the fraction X of RC's which show no electron transfer past A_1 has been set to 0.20 and the fraction Y of RC's in which the transfer to F_X is faster than the response time of the spectrometer has been set to 0.60 (see the text).

emission due to $P_{700}^{+\bullet}(FeS)^-$ at early times. This effect is immediately apparent in transients from the two spinach samples shown in Figure 3. In the PS I-β particle sample (Figure 3, bottom) which is known to have a large fraction of reaction centers with $t_{1/2} = 25$ ns the intensity of the early absorption is very weak compared to the emission at later times. In contrast, in the chloroplast sample (Figure 3, bottom) the early absorption is much stronger. Note, however, that this difference is exaggerated by the different microwave powers used for the two samples.

The spin-polarized EPR transients and spectra shown Figures 1–4 clearly contain information regarding the pathway and kinetics of the electron transfer past A_1. However, it is equally clear that the method of preparation and species used leads to differences in the signals. Thus, in order to draw conclusions about the electron transfer kinetics under physiological conditions in fully intact PS I, it is important to consider these differences in more detail. In the following we will describe a kinetic model which can be used to separate the various contributions to the EPR signals and will then discuss the rate constants for the electron transfer past

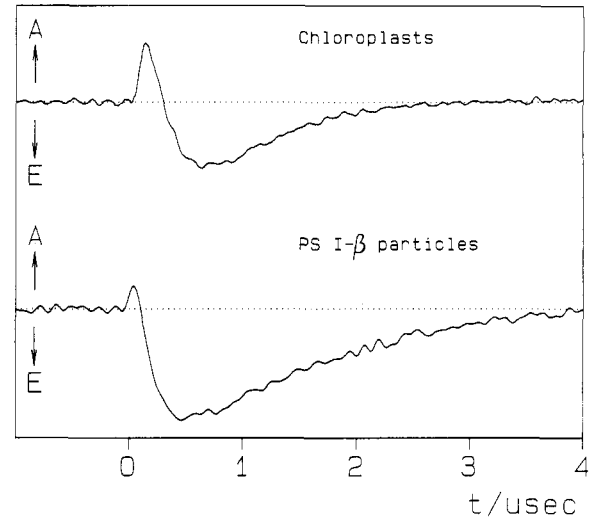

FIGURE 3: Transient EPR signals from PS I in spinach in the region 338.725–338.975 mT at room temperature. The field position is marked with an arrow in the corresponding spectra shown in Figure 4. Top trace: chloroplasts; microwave power, 40 mW; microwave frequency, 9.507 GHz; average of 7680 events. Bottom trace: PS I-β particles; microwave power, 10 mW; microwave frequency, 9.5052 GHz; average of 7680 events. In both cases the signal has been filtered with a 10 MHz low-pass filter. The time $t = 0$ is defined as in Figure 1.

$A_1^{-\bullet}$ and spectra of the charge-separated states obtained from the data of the various samples using the model. This analysis will show that in unperturbed PS I samples the electron transfer from $A_1^{-\bullet}$ to the iron–sulfur centers proceeds via F_X with $t_{1/e} \approx 280$ ns ($t_{1/2} \approx 190$ ns) and that the faster electron transfer kinetics observed in some particle preparations is apparently a result of the preparation procedure.

Analysis of PS I Subpreparations

The goal of the analysis is to extract from the data the rate constants for the various processes which influence the EPR signals as well as the spin-polarized EPR spectra of the charge separated states involved. This requires a general description which can then be reduced to the specific cases encountered for the various samples. The treatment of the data follows essentially the same approach as used by Bock et al. (1989). However, we have generalized the description of the transients rather than using the somewhat *ad hoc* function given by Bock et al. (1989). The transient EPR signal of a sample containing several light-induced paramagnetic species is a function of magnetic field strength, B_0, and time, t, and can be written as

$$S(t,B_0) = \sum_i S_i(t,B_0) \tag{1}$$

The signal of a given species $S_i(B_0,t)$ depends on the evolution with time of its concentration and spin polarization. For the reaction $A^{-\bullet} \rightarrow B^{-\bullet}$, we obtain

$$S_A(t,B_0) = \alpha(B_0)e^{-(k+w_A)t} \tag{2}$$

$$S_B(t,B_0) = \beta(B_0)\frac{k}{k + w_A - w_B}\{e^{-w_B t} - e^{-(k+w_A)t}\} \tag{3}$$

where k is the first-order reaction rate constant, w_A and w_B are the decay rates of the spin polarization in species $A^{-\bullet}$ and $B^{-\bullet}$, respectively, and $\alpha(B_0)$ and $\beta(B_0)$ are their spin-polarized EPR spectra in the absence of relaxation. For similar PS I

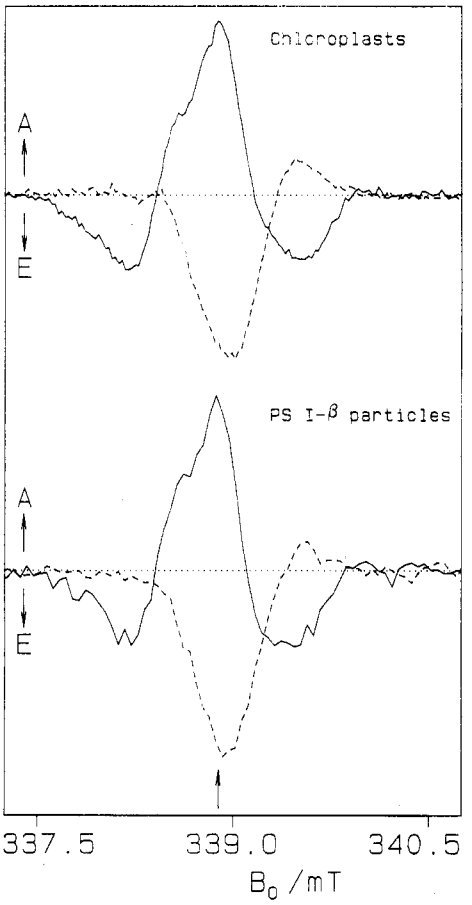

FIGURE 4: Transient EPR spectra derived from the data sets from spinach PS I samples. The arrow indicates the field position for the transients in Figure 3. The spectra have been obtained by fitting eq 4 to the experimental transients: solid curves, early spectrum $\alpha(B_0)$; dashed curves, late spectrum $\beta(B_0)$. The rate constants used are given in Table 1. The spectrometer response time is 50 ns in all cases. The top spectra are from the chloroplast sample and the bottom spectra are from PS I-β particles. In the bottom trace the fraction Y of RC's in which the electron transfer is faster than the response time is 0.45 (see the text).

preparations, it was shown by Bock et al. (1989) how the decay of the spin polarization depends on the microwave power. The decay is given by the spin–lattice relaxation rate in the limit-zero microwave power (Atkins et al., 1973; Pedersen, 1973; Furrer et al., 1980). For finite values of the microwave power, w_A and w_B are effective relaxation rates and are shorter than the corresponding spin–lattice relaxation rates. In eqs 2 and 3 we have made no assumptions about the relative magnitudes of k, w_A, and w_B. This is in contrast to the work of Bock et al. (1989), where the relaxation has not been taken into account correctly and the equation used is only valid if the two effective relaxation rates are negligible compared to the reaction rate. Although it is reasonable to make this approximation for the signals from PS I, it will have an influence on the values of k, w_A, and w_B obtained from the data. If these rate constants are much smaller than the inverse of the spectrometer response time, then eqs 2 and 3 will accurately represent the measured signals. In the present case, the response function is a simple exponential with an inverse rate constant of $\sim$50 ns whereas $k^{-1} \approx 200$ ns. Thus, this condition is not well fulfilled and the response of spectrometer should be taken into account. This can be done by calculating the convolution integral of the response function and the EPR signal. In addition we should also include two fractions, X and Y, to take into account those RC's in which the electron transfer past A_1 is blocked and those which show electron transfer to the iron–sulfur centers with a rate constant, k', which is faster than the rise time of the spectrometer. This leads to the following expression:

$$S_{obs}(t,B_0) = \gamma(B_0)(1-X-Y)\{e^{-(w_A+k)t} - e^{-k_i t}\} + \gamma'(B_0)Y\{e^{-(w_A+k')t} - e^{-k_i t}\} + \alpha(B_0)X\{e^{-w_A t} - e^{-k_i t}\} + \{\delta(B_0)(1-X-Y) + \delta'(B_0)(Y)\}\{e^{-w_B t} - e^{-k_i t}\} \quad (4)$$

where k_i is the inverse of the spectrometer response time, $b = k/(w_A + k - w_B)$, $\gamma(B_0) = [(\alpha(B_0) - b\beta(B_0))k_i/(k_i - w_A - k)$, and $\delta(B_0) = (k_i b\beta(B_0))/(k_i - w_B)$. $\gamma'(B_0)$ and $\delta'(B_0)$ are identical to $\gamma(B_0)$ and $\delta(B_0)$ except that k is replaced by k'.

Kinetics of the Electron Transfer past A_1

In order to obtain values for the rate constants and amplitudes, eq 4 has been fitted to the experimental transients using a least squares procedure. A global fit involving all of the rate constants and experimental curves is not possible because of the large number of variables involved. Thus, we have fixed the values of the rate constants as follows. First, the rise time of the spectrometer, k_i^{-1} has been estimated from the response of the resonator to suddenly (<10 ns) switching on the microwave power. The value of 50 ns for k_i^{-1} has been kept constant throughout. The value of w_A, which is the effective relaxation time for species A (in this case $P_{700}^{+\bullet}A_1^{-\bullet}$), has been obtained by fitting eq 4 to the transients from the (P_{700}-A_1) core sample in which all iron–sulfur have been removed and no electron transfer past $A_1^{-\bullet}$ takes place, i.e. the fraction $X = 1$. For the other samples, w_A has little effect on the results provided that it is more than roughly a factor of 2 smaller than k. Here, we have assumed that it is the same in all samples. The value of w_B has then been obtained from a fit to the transients around $B_0 = 338.85$ mT ($g = 2.0040$), which are shown in Figures 1 and 3 for several samples. The rate constant k' for the fast electron transfer can be obtained from transient optical absorption measurements as described by Sétif and Brettel (1993). The fraction Y of centers in which the electron transfer is governed by k' can also be estimated from the form of the spectrum $\alpha(B_0)$ (see below). The fraction X of centers in which the electron transfer past A_1 is blocked can be determined by fitting the transients on the low field side of the EPR spectrum. Having fixed the values of w_A, w_B, k', X, and Y, the electron transfer rate k can then be determined at those field positions with sufficient signal strength. Although a certain amount of scatter is observed in the values of k obtained at different magnetic field positions, there are no systematic variations.

The rate constants obtained from the fits are collected in Table 1. For all samples containing iron–sulfur centers the value of k^{-1} is roughly 280 ns, and with the exception of the (P_{700}-F_X) core particles, w_B^{-1} is 1.4 μs. The electron transfer rates shown in Table 1 are slightly slower than those from corresponding samples reported by Bock et al. (1989). However, this is expected since the latter rates contain a contribution from the relaxation in the pair $P_{700}^{+\bullet}A_1^{-\bullet}$.

Cyanobacterial Samples. Of particular interest is the sample in which the PsaC protein has been removed. In this sample, the transients at magnetic field values around $B_0 = 338.10$ mT ($g = 2.0083$), where the only contribution to the spin-polarized EPR signal is from the radical pair $P_{700}^{+\bullet}A_1^{-\bullet}$, are biexponential and can be fitted with $X = 0.21$, in reasonable agreement with the value of 0.35 obtained from the transient optical absorption traces at 380 and 811 nm (data not shown). Thus we conclude that the treatment used to remove the PsaC

Table 1: Electron Transfer and Relaxation Times in Various PS I Preparations[a]

sample	k^{-1} (ns)		w_A^{-1} [b] (ns)		w_B^{-1} [b] (ns)	
	$t_{1/e}$	$t_{1/2}$	$t_{1/e}$	$t_{1/2}$	$t_{1/e}$	$t_{1/2}$
Synechococcus 6301						
whole cells	270	190	*c*	*c*	1330	920
thylakoid membranes	290	200	*c*	*c*	1390	960
(P_{700}-F_A/F_B) DM	270	190	*c*	*c*	1470	1010
(P_{700}-F_A/F_B) Triton X-100	320	220	*c*	*c*	1660	1150
(P_{700}-F_X) core	300	210	*c*	*c*	3960	2740
(P_{700}-A_1) core			1360	940		
Synechococcus sp.	290	200	*c*	*c*	1330	920
Synechocystis 6803	290	200	*c*	*c*	1640	1140
spinach						
chloroplasts	290	200	*c*	*c*	790	550[d]
digitonin particles	260	180	*c*	*c*	1670	1160
PS I-β particles	290	200	*c*	*c*	1640	1130

[a] Estimated error in all values ±20%. [b] Effective relaxation times for microwave power = 10 mW. [c] Value assumed to be the same as for *Synechococcus* (P_{700}-A_1) core sample. [d] Microwave power = 40 mW.

protein (see Materials and Methods) has also removed F_x in about 30% of the RC's. Using this value it is then possible to fit the transients at other field positions. Surprisingly the value of w_B^{-1} obtained from these fits is roughly a factor two larger than that found for the other samples. Nonetheless, it is apparent that the electron transfer time of $t_{1/e} \approx 280$ ns ($t_{1/2} \approx 190$ ns) is retained even though F_A and F_B have been removed. In contrast to this, when F_x is removed from the RC no electron transfer beyond A_1 is observed in the spin polarized EPR signals. Thus, in the (P_{700}-F_X) core sample we can assign the 280 ns rate constant to the electron transfer reaction:

$$P_{700}^{+\bullet}A_1^{-\bullet} \xrightarrow{280\ \text{ns}} P_{700}^{+\bullet}F_X^{-} \qquad (5)$$

With the exception of the (P_{700}-A_1) core sample in which F_X has been removed, the same rate constant is observed in all other cyanobacteria samples studied including whole cells. This suggests that it is also reaction 5 which occurs in intact PS I in cyanobacteria under physiological conditions.

Spinach Samples. The transient EPR signals for the spinach samples (Figure 3) are qualitatively similar to those obtained from the cyanobacteria and yield rate constants (see Table 1 and Bock et al., 1989) which are consistent with the optical results for these samples (Brettel, 1989; Sétif & Brettel, 1993). However, the optical data also show that the reoxidation of $A_1^{-\bullet}$ in PS I particles from spinach is biphasic and that the fraction Y of RC's in which it occurs with $t_{1/2} = 25$ ns ($t_{1/e} = 36$ ns) is ~0.65 (Sétif & Brettel, 1993). The intensity ratio of the two species $\alpha(B_0)/\beta(B_0)$ also gives a qualitative measure of the fraction Y in various samples. At the field position shown in Figure 3, we obtain values of –0.82 and –0.39 for the chloroplast and PS I-β samples, respectively, in reasonable agreement with the optical results. Because this ratio could in principle be influenced by the microwave power, it was studied using the *Synechococcus* sp. particle sample and values of –0.95 and –0.85 were obtained at 10 and 50 mW, respectively. Thus, we can conclude that the large difference in $\alpha(B_0)/\beta(B_0)$ observed in the two spinach samples results from the fact that the fraction Y is much smaller in the chloroplasts.

EPR Spectra and Electron Transfer Pathway past A_1

The transient EPR data also provide information about the identity of the electron acceptors and thus about the pathway of the electron transfer. The coefficients $\alpha(B_0)$ and $\beta(B_0)$ in eq 4 are the spin-polarized EPR spectra of the two sequential radical pairs $P_{700}^{+\bullet}A_1^{-\bullet}$ and $P_{700}^{+\bullet}(FeS)^-$. The spectra can in principle be used to identify the first acceptor following $A_1^{-\bullet}$. A straightforward assignment of the $P_{700}^{+\bullet}(FeS)^-$ spectrum based on the g-factors of the iron–sulfur centers is not possible because the contribution to the spectrum from $(FeS)^-$ is not visible. This occurs because the large anisotropy in the iron–sulfur center g-tensors distributes the intensity over a large spectral range. Nonetheless, we expect changes in the spectrum $\beta(B_0)$ depending on which of the iron–sulfur centers accepts the electron from $A_1^{\bullet-}$, because the spectrum is also determined by the distance between the donor and acceptor as well as their orientations relative to one another. The spectra corresponding to the various species have been obtained by fitting all transients in the data set using the rate constants given in Table 1 and varying only the amplitudes $\alpha(B_0)$ and $\beta(B_0)$.

Influence of the $t_{1/e} = 35$ ns ($t_{1/2} = 25$ ns) Phase on the EPR Spectra. In order to demonstrate the effect of the $t_{1/e} = 35$ ns ($t_{1/2} = 25$ ns) component on the form of the spectra, we have fitted the data set from the *Synechococcus* sp. PS I particle sample also presented by Bock et al. (1989). Here, we have used eq 4 with different values of the fraction of centers Y the rate of which electron transfer to the iron–sulfur centers is faster than the response of the spectrometer. The resulting spectra are shown in Figure 5. In the top part of the figure, the spectra obtained with $Y = 0$ are shown. The solid curve is the spectrum $\alpha(B_0)$ and the dashed curve is $\beta(B_0)$. In the bottom part of the figure the spectra $\alpha(B_0)$ are shown for $Y = 0$ (solid curve), $Y = 0.2$ (dashed curve), and $Y = 0.4$ (dotted curve). The corresponding late spectra $\beta(B_0)$ are independent of Y and thus are not shown. Introducing the fraction, Y effectively reduces the contribution from $\alpha(B_0)$ to $S(t,B_0)$ at $t = 0$. Which is equivalent to reducing the concentration of centers which are in the state $P_{700}^{+\bullet}A_1^{-\bullet}$ at the earliest time which can be detected with the spectrometer. In order to take this difference in concentration into account, the spectra shown in Figure 5 (bottom) have been scaled by a factor of $1 - Y$. As can be seen, taking the $t_{1/e} = 35$ ns ($t_{1/2} = 25$ ns) component into account leads to an increase in the intensity of $\alpha(B_0)$ at those field positions where $\beta(B_0)$ is also present and of opposite sign. It should be kept in mind that the quality of the fits that leads to all three spectra is identical and does not provide a criterion for determining Y. However, the spectrum $\alpha(B_0)$ should be that of a correlated, coupled radical pair generated suddenly from a singlet precursor. The absorptive and emissive contributions to such a spectrum are equal and opposite and the net spin polarization is zero (Thurnauer & Norris, 1980; Thurnauer & Meisel, 1983; Hore et al., 1987; Buckley et al., 1987; Closs et al., 1987; Stehlik et al., 1989a; Norris et al., 1990; Hore, 1989; Bixon et al., 1992; Snyder & Thurnauer, 1993). This fact can be used to estimate the value of Y. Introducing Y adds a primarily emissive contribution from $P_{700}^{+\bullet}(FeS)^-$ at early times. Thus, if Y is taken to be too large or too small, it will be compensated for in the fit by adding absorptive or emissive intensity, respectively, to $\alpha(B_0)$. Integration of the spectra $\alpha(B_0)$ in Figure 5 (bottom) shows that the net polarization depends roughly linearly on the value of Y and is zero for $Y \approx 0.15$. Considering the number of assumptions and parameters involved in this estimation, it is in good agreement with the estimate of $Y < 0.15$ obtained from optical transients of these particles (Brettel, 1989; Sétif & Brettel, 1993).

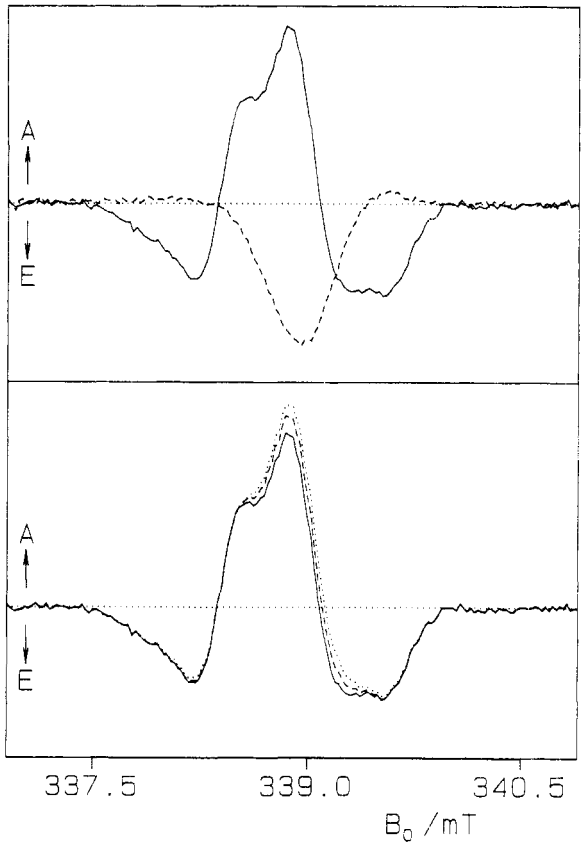

FIGURE 5: Transient EPR spectra derived from the time/magnetic field data set of PS I particles from *Synnechococcus* sp. at 10 mW microwave power presented by Bock et al. (1989). All spectra have been obtained by fitting eq 4 to the respective experimental transients. (top) The solid and dashed curves are the early spectrum $\alpha(B_0)$ and late spectrum $\beta(B_0)$, respectively. It is assumed that the fraction Y of RC's in which the electron transfer is faster than the response time is zero (see the text). The rate constants used are given in Table 1. The spectrometer response time is 50 ns in all cases. (bottom) The dependence of the early spectrum on Y. The solid, dashed, and dotted curves are for $Y = 0$, 0.2, and 0.4, respectively.

In Figure 4 the spectra obtained from spinach chloroplasts (top) and PS I-β particles (bottom) are shown. The fraction Y has been chosen so that the early spectra $\alpha(B_0)$ show no net polarization and is zero for the chloroplasts and 0.6 for the PS I-β particles. As can be seen in Figure 4 the spectra from the two samples are virtually indistinguishable. From these results it is clear that in spinach chloroplasts fast electron transfer ($t_{1/e} < 50$ ns, $t_{1/2} < 35$ ns) to the iron–sulfur centers does not occur to any significant extent whereas a considerable fraction of the PS I-β particles do show such a fast electron transfer. The value of 0.6 for this fraction is in good agreement with the more accurate estimate of 0.65 from optical measurements on the same particles (Sétif & Brettel, 1993).

Influence of the Number of Acceptors on the EPR Spectra. In Figure 2 the spectra derived from the data sets from (P_{700}-F_A/F_B) DM particles, (P_{700}-F_X) core particles, and (P_{700}-A_1) core particles are presented. (The corresponding transients are shown in Figure 1.) In all three samples, the early spectrum $\alpha(B_0)$ (solid curves) has the well-known E/A/E polarization pattern which is characteristic of spin-coupled correlated RP's and the late spectra, where present (dotted curves), are all predominantly emissive and centered around $g = 2$ ($B_0 =$ 339.0 mT). However, closer inspection of the spectra reveals differences between the various samples.

Samples Containing F_A/F_B. The spectra in Figure 2 (top) are from the (P_{700}-F_A/F_B) DM particle sample. Identical spectra are obtained from the other cyanobacterial samples containing F_A/F_B, provided that the fraction Y of centers showing a fast electron transfer to the iron–sulfur centers is chosen so that the early spectrum shows no net polarization. An exception is the early spectrum from the whole cell sample (not shown), which is probably different as a result of a flow-induced orientation of the sample (Dismukes et al., 1978). As with the spinach PS I samples, the fraction Y depends on the method of preparation. In the case of the thylakoid membranes and (P_{700}-F_A/F_B) DM particles, a value of $Y = 0.15$ was used. However, for the Triton X-100 sample, a value of $Y = 0.32$ is obtained. Again, this value is in good agreement with the optical data from the particle samples (Brettel, K. and Goldbeck, J. unpublished results; Lüneberg, J., Schlodder, E., and Goldbeck, J. unpublished results) and are analogous to the results in spinach. From this we can immediately make two important conclusions: (i) A $t_{1/e} < 50$ ns ($t_{1/2} < 35$ ns) component in the electron transfer to the iron–sulfur centers can occur in cyanobacterial PS I as well as in spinach PS I and (ii) it is apparently a result of the procedure used to isolate the PS I complex from the thylakoid membranes and depends on which detergent is used.

As can be seen by comparing Figures 2, 4, and 5 (top) the early spectra from all samples containing F_A/F_B are identical. However, despite the fact that the kinetic behavior of the spinach and cyanobacterial PS I samples is very similar, the form of their late spectra is different. The late spectra from the two spinach samples have an absorptive contribution on their high field side whereas in the corresponding spectra from the cyanobacterial (P_{700}-F_A/F_B) particles (see Figures 2 and 5, top) this feature is much weaker and the whole spectrum is slightly broader.

Samples Containing F_X but Not F_A/F_B. The analysis of the transient EPR data set from the (P_{700}-F_X) core particles requires considerable care because it is obvious from the decay curves that the sample is not homogeneous. The relative concentrations of RC's associated with the various kinetic phases in the sample can be deduced independently from the optical transients at 811 and 380 nm. From these transients (not shown) it is estimated that (i) in 48% of the RC's the electron transfer from $A_1^{-\bullet}$ to F_X occurs with $t_{1/e} \approx 36$ ($t_{1/2} \approx 25$ ns), (ii) in 32% of the RC's it occurs with $t_{1/e} \approx 260$ ns ($t_{1/2} \approx 180$ ns) and (iii) in 20% of the RC's no transfer past A_1 takes place. The EPR signal from $P_{700}^{+\bullet}A_1^{-\bullet}$ is dominated by the latter two fractions. Thus, the optical data predict that 38% of this signal should decay with the spin polarization decay rate w_A. This prediction agrees fairly well with the value of ~20% determined by fitting the transients on the low field side of the EPR spectrum where $P_{700}^{+\bullet}(FeS)^-$ does not contribute.

The EPR spectra $\alpha(B_0)$ and $\beta(B_0)$ for this sample using eq 4 and the parameters given in Table 1 are shown in Figure 2 (Middle). The early spectrum (solid curve) shows no net polarization and is indistinguishable from the early spectrum from the spinach and cyanobacterial samples containing F_A/F_B. From these results we can conclude that (i) both the $t_{1/2} \approx 180$ ns and $t_{1/2} \approx 25$ ns phases can be assigned to the electron transfer from $A_1^{-\bullet}$ to F_X, which provides strong evidence that, under physiological conditions in intact PS I, F_X is the first electron acceptor following A_1 and (ii) the magnetic and structural parameters which describe the spectrum of $P_{700}^{+\bullet}A_1^{-\bullet}$ are independent of which species (cyanobacteria or spinach) is studied and whether F_A/F_B is present or not.

The late spectrum $\beta(B_0)$ from (P_{700}-F_X) core particles (Figure 2, middle, dashed curve) shows small but significant

differences compared to the corresponding spectrum from the cyanobacterial samples containing F_A/F_B (Figure 2, top). A weak absorption is observed on the high field side of the spectrum, whereas in the spectra from the cyanobacterial samples containing F_A/F_B this feature is missing and the spectrum is slightly broader. Since the spectrum of $P_{700}^{+\bullet}A_1^{-\bullet}$ is identical in all of these samples, a change in $P_{700}^{+\bullet}$ can be ruled out and the differences in the late spectrum must result from changes related to the iron–sulfur centers. Calculations of correlated coupled radical pair spectra (Füchsle et al., 1993) show that small changes in the magnetic parameters and geometry of the charge-separated state can induce rather large changes in the spectra. Thus it is reasonable to expect that removal of the PsaC protein causes differences in the late spectrum. It is also conceivable that the electron transfer from F_X^- to (F_A/F_B) is very fast so that in the $(P_{700}\text{-}F_A/F_B)$ particles the late spectrum is due to $P_{700}^{+\bullet}(F_A/F_B)^-$.

Samples Containing No Iron–Sulfur Centers. The spectrum extracted from the EPR data set from $(P_{700}\text{-}A_1)$ core particles is shown in Figure 2 (bottom). In this case only one charge separated state is observed and the transients can be fitted with eq 4 with $X = 1$ and $Y = 0$. This spectrum can clearly be assigned to the radical pair $P_{700}^{+\bullet}A_1^{-\bullet}$; however, it is significantly different from the corresponding spectra from the samples containing iron–sulfur centers. In particular, the shoulder on the low field side of the central absorptive peak is missing. This feature is not observed in the X-band spectra of fully deuterated PS I (Stehlik et al., 1989a; Kothe et al., 1991) nor in the K-band (24 GHz) spectrum of protonated PS I particles (Füchsle et al., 1993), which suggests that it might be due to proton hyperfine couplings. If this is correct, then the disappearance of this feature when F_X is removed from the RC could be due to a reduction in the hyperfine couplings in $A_1^{-\bullet}$ as a result of changes in the protein environment.

CONCLUSIONS

The results presented here show that forward electron transfer past A_1 is blocked when all three iron–sulfur centers, F_X, F_A, and F_B, are removed from the PS I reaction center. However, no change in the rate of reoxidation of $A_1^{-\bullet}$ is observed if only the PsaC protein containing F_A/F_B is removed. This provides convincing evidence that the electron acceptor following A_1 is F_X. In addition, the EPR data from spinach chloroplasts, cyanobacterial cells, and thylakoid membranes (i.e. those samples which have undergone the least amount of chemical treatment) do not show any indication of a $t_{1/e} \approx 35$ ns ($t_{1/2} \approx 25$ ns) phase in the electron transfer from $A_1^{-\bullet}$ to F_X. In contrast, such a phase is clearly evident in the optical and EPR results for many PS I particle preparations from both spinach and cyanobacteria. The size of the fraction of RC's which show such kinetics depends on the method of preparation and is particularly large in those samples prepared using Triton X-100. From this we conclude that in PS I in intact cells under physiological conditions the electron transfer past A_1 is to F_X and proceeds with a transfer time of $t_{1/e} \approx 280$ ns ($t_{1/2} \approx 190$ ns).

ACKNOWLEDGMENT

A.v.d.E. wishes to thank R. Bittl for useful discussions about the numerical analysis and A. Kamlowski for proofreading the manuscript.

REFERENCES

Andreasson, L. E., & Vänngard, T. (1988) *Annu. Rev. Plant Physiol. Plant Mol. Biol. 39*, 379–411.
Atkins, P. W., McLauchlan, K. A., & Percival, P. W. (1973) *Mol. Phys. 25*, 281–296.
Bixon, M., Fajer, J., Feher, G., Freed, J. H., Hoff, A. J., Levanon, H., Möbius, K., Nechustai, R., Norris, J. R., Scherz, A., Sessler, J. L., & Stehlik, D. (1992) *Isr. J. Chem. 32*, 369–518.
Bock, C. H. (1989) Ph.D. Thesis, Free University, Berlin.
Bock, C. H., van der Est, A. J., Brettel, K., & Stehlik, D. (1989) *FEBS Lett. 247*, 91–96.
Brettel, K. (1989) *FEBS Lett. 239*, 93–98.
Buckley, C. D., Hunter, D. A., Hore, P. J., & McLauchlan, K. A. (1987) *Chem. Phys. Lett. 135*, 307–312.
Closs, G. L., Forbes, M. D. E., & Norris, J. R. (1987) *J. Phys. Chem. 91*, 3592–3599.
Dismukes, G. C., McGuire, A., Blankenship, R., & Sauer, K. (1978) *Biophys. J. 21*, 239–256.
Füchsle, G., Bittl, R., van der Est, A., Lubitz, W., & Stehlik, D. (1993) *Biochim. Biophys. Acta 1142*, 23–35.
Furrer, R., Fujara, F., Lange, C., Stehlik, D., Vieth, H. M., & Vollmann, W. (1980) *Chem. Phys. Lett. 75*, 332–339.
Golbeck, J. (1992) *Annu. Rev. Plant Physiol. Plant Mol. Biol. 43*, 293–324.
Golbeck, J. H., & Cornelius, J. M. (1986) *Biochim. Biophys. Acta 849*, 16–24.
Golbeck, J. H., Parrett, K. G., & McDermott, A. E. (1987) *Biochim. Biophys. Acta 893*, 149–160.
Heathcote, P., Hanley, J., & Evans, M. (1993) *Biochim. Biophys. Acta 1144*, 54–61.
Holzwarth, A., Schatz, G., Brock, H., & Bittersmann, E. (1993) *Biophys. J. 64*, 1813–1826.
Hore, P. J. (1989) in *Advanced EPR, Applications in Biology and Biochemistry* (Hoff, A. J., Ed.) Chapter 12, pp 405–440, Elsevier, Amsterdam.
Hore, P. J., Hunter, D. A., McKie, C. D., & Hoff, A. J. (1987) *Chem. Phys. Lett. 137*, 495–500.
Kothe, G., Weber, S., Bittl, R., Ohmes, E., Thurnauer, M. C., & Norris, J. R. (1991) *Chem. Phys. Lett. 186*, 474–480.
Kratz, W. A., & Myers, J. (1955) *Am. J. Bot. 42*, 282–287.
Lagoutte, B., & Mathis, P. (1989) *Photochem. Photobiol. 49*, 833–844.
Lagoutte, B., Sétif, P., & Duranton, J. (1984) *FEBS Lett. 174*, 24–29.
Lüneberg, J., Fromme, P., Jekow, P., & Schlodder, E. (1994) *FEBS Lett. 338*, 197–202.
Malkin, R., & Bearden, A. J. (1971) *Proc. Natl. Acad. Sci. U.S.A. 68*, 16–19.
Mathis, P., & Sétif, P. (1989) *FEBS Lett. 237*, 65–68.
Norris, J. R., Morris, A. L., Thurnauer, M. C., & Tang, J. (1990) *J. Chem. Phys. 92*, 4239–4249.
Parrett, K. G., Mehari, T., Warren, P., & Golbeck, J. H. (1989) *Biochim. Biophys. Acta 973*, 324–332.
Parrett, K. G., Mehari, T., & Golbeck, J. H. (1990) *Biochim. Biophys. Acta 1015*, 341–352.
Pedersen, J. B. (1973) *J. Chem. Phys. 59*, 2656–2667.
Rustandi, R. R., Snyder, S. W., Feezel, L. L., Michalski, T. J., Norris, J. R., Thurnauer, M. C., & Biggins, J. (1990) *Biochemistry 29*, 8030–8032.
Rustandi, R. R., Snyder, S. W., Biggins, J., Norris, J. R., & Thurnauer, M. C. (1992) *Biochim. Biophys. Acta 1101*, 311–320.
Sétif, P. (1992) in *The Photosystems: Structure, Function and Molecular Biology* (Barber, J., Ed.) Chapter 12, pp 471–499, Elsevier, Amsterdam.
Sétif, P., & Brettel, K. (1993) *Biochemistry 32*, 7846–7854.
Sieckmann, I., van der Est, A., Bottin, H., Sétif, P., & Stehlik, D. (1991) *FEBS 284*, 98–102.
Snyder, S. W., & Thurnauer, M. C. (1993) in *The Photosynthetic Reaction Center* (Norris, J. R., & Deisenhofer, J., Eds.) Vol. II, pp 285–331, Academic Press, New York.

Snyder, S. W., Rustandi, R. R., Biggins, J., Norris, J. R., & Thurnauer, M. C. (1991) *Proc. Natl. Acad. Sci. U.S.A. 88*, 9895–9896.

Stehlik, D., Bock, C. H., & Petersen, J. (1989a) *J. Phys. Chem. 93*, 1612–1619.

Stehlik, D., Bock, C. H., & Thurnauer, M. C. (1989b) in *Advanced EPR Applications in Biology and Biochemistry* (Hoff, A. J., Ed.) Chapter 11, pp 370–403, Elsevier, Amsterdam.

Stehlik, D., Sieckmann, I., & van der Est, A. (1993) in *Research in Photosynthesis: Proceedings of the IX th International Congress on Photosynthesis* (Murata, N., Ed.) pp 533–536, Kluwer Acad. Publ., Dordrecht.

Thurnauer, M. C., & Meisel, D. (1983) *J. Am. Chem. Soc. 105*, 3729–3731.

Thurnauer, M. C., & Norris, J. R. (1980) *Chem. Phys. Lett. 76*, 557–561.

Warden, J. T., & Golbeck, J. H. (1986) *Biochim. Biophys. Acta 849*, 25–33.

Warren, P. V., Parrett, K. G., & Golbeck, J. H. (1990) *Biochemistry 29*, 6545–6550.

Warren, P. V., Golbeck, J. H., & Warden, J. T. (1993) *Biochemistry 32*, 849–857.

Winget, G. D., Izawa, S., & Good, M. E. (1965) *Biochem. Biophys. Res. Commun. 21*, 439–443.